Electronic Supplementary Material (ESI) for Nanoscale.

Supporting Information

Soft-Template Assisted Synthesis of Hexagonal Antimonene and Bismuthene in Colloidal Solutions

Jing Zhang, Shuai Ye,* Yuan Sun, Feifan Zhou, Jun Song, and Junle Qu

Center for Biomedical Optics and Photonics (CBOP) & College of Physics and Optoelectronic Engineering, Key Laboratory of Optoelectronic Devices and Systems, Shenzhen University, Shenzhen 518060, P. R. China

Email: yes-121@163.com or yes121@szu.edu.cn

Table of contents

Experimental Section		S2
Figure S1.	Photograph and XRD pattern of Sb_2S_3 synthesized by Sb-DDT	S4
Figure S2-1.	The TEM images of synthesized antimonene at 250 and 230 °C	S5
Figure S2-2.	AFM image of antimonene nanosheets	S5
Figure S2-3.	EDS spectrum of antimonene nanosheets	S6
Figure S2-4.	Wide-scan XPS spectrum of antimonene nanosheets	S6
Figure S2-5.	The absorption spectrum of synthesized antimonene nanosheets	S7
Figure S3-1.	XRD pattern of synthesized antimonene nanosheets after storage	S8
Figure S3-2.	The TEM images of synthesized antimonene nanosheets after storage	S8
Figure S3-3.	XPS spectrum of synthesized antimonene nanosheets after storage	S9
Figure S3-4.	TGA analysis of synthesized antimonene nanosheets	S9
Figure S4-1.	The TEM images of Sb nanocrystals synthesized with Sb-TOPO	S10
Figure S4-2.	XRD pattern of Sb nanocrystals synthesized with Sb-TOPO	S10
Figure S5-1.	Small-angle XRD pattern of Sb-HPA and TEM image of products	S11
Figure S5-2.	Small-angle XRD pattern of Sb-DDT precursor	S11
Table S1.	Calculation of interlayer spacing in lamellar structure and ligand length.	S12
Figure S6-1.	EDS spectrum of bismuthene nanosheets	S13
Figure S6-2.	Wide-scan XPS spectra of bismuthene nanosheets	S13
Figure S6-3.	The absorption spectrum of synthesized bismuthene nanosheets	S14
Figure S6-4.	Stability test of synthesized bismuthene nanosheets	S14

EXPERIMENTAL SECTION

Chemicals. Antimony trichloride ($SbCl_3$, 99.999%), antimony triacetate ($Sb(OAc)_3$, 99.99%), hexylphosphonic acid (HPA, 95%), trioctylphosphine oxide (TOPO, 99%), 1-dodecanethiol (1-DDT, 99.9%), and oleylamine (OLA, 70%) were purchased from Sigma Aldrich. Bismuth trichloride ($BiCl_3$, 99.99%) and hexadecylphosphonic acid (HDPA, 98%) were purchased from Macklin, dodecylphosphonic acid (DDA, 98%) was purchased from Aladdin. Cyclohexane, ethanol, toluene and chloroform were used as received.

Synthesis of antimonene and bismuthene nanosheets.

In a typical reaction batch for synthesizing antimonene nanosheets (Figure 1), Sb precursors were prepared first. $SbCl_3$ (0.137 g, 0.6 mmol) and HDPA (0.721 g, 2.0 mmol) were loaded into a glass vial at room temperature followed by reacting at 90 °C to get a colorless Sb precursor solution. 4.5 mL OLA was degassed in a 50 mL three-necked flask at room temperature for 30 min. Afterwards, the solution was heated up to 270 °C under nitrogen and Sb precursors solution was swiftly added into the OLA solution with immediately formation of gray suspension. After 1 min of growth, the heating mantle was removed to quench the reaction. The as-synthesized samples were quickly extracted from the reaction flask for further washing when the solution temperature decreased to 120 °C. For the synthesis of bismuthene nanosheets (Figure 4), Bi precursor was prepared through a similar way through reacting between $BiCl_3$ (0.190 g, 0.6 mmol) and DDA (0.501 g, 2.0 mmol) at 90 °C.

To wash the samples, we extracted the crude samples and centrifuged at 8000 rpm for 5 s. The supernatant was discarded, and the precipitates were dispersed in toluene followed by sonicating for 5 mins. Afterwards, the solutions were centrifuged at 8500 rpm for 2 min. We repeated this process for five times to get purified samples. Finally, the samples were dispersed in toluene for further characterization.

Preparation of Sb-HPA, Sb-TOPO and Sb-DDT precursors: For investigating the lamellar structure of Sb precursors, we prepared Sb-HPA and Sb-TOPO precursors by reacting $SbCl_3$ (0.137 g, 0.6 mmol) with HPA (0.332 g, 2.0 mmol) at 80 °C (Figure 3c), and TOPO (0.773 g, 2.0 mmol) at 50 °C (Figure 3e). Moreover, Sb-DDT was also prepared (Figure S5-2) through

mixing $Sb(OAc)_3$ (0.137 g, 0.6 mmol) and 1-DDT (0.50 mL, 2.0 mmol) at 50 °C.

Characterization.

The purified samples were dispersed in toluene and dropped on a carbon coated copper grid for TEM characterization. Transmission electron microscope (TEM) images and Energy-dispersive spectroscopy (EDS) measurements were performed on a transmission electron microscope (JEM-F200, JEOL) with an acceleration voltage of 200 kV. The low-resolution TEM images in supporting information were collected on a HT7700 transmission electron microscope.

UV-visible absorption spectra were collected with 1 nm date collection interval by a SHIMADZU UV-1780 UV-visible spectrophotometer. Powder X-ray diffraction (XRD) patterns were recorded on an X-ray diffractometer (Ultima IV) with a Cu Kα beam (λ = 1.5418 Å), the purified samples were dispersed in cyclohexane and deposited on a silicon substrate for XRD test. X-ray photoelectron spectroscopy (XPS) measurements were performed using PHI5000VersaProbell, with the purified antimonene and bismuthine nanosheet samples dropped on silicon wafer. Raman spectra were collected using a Confocal Raman Microscope (Alpha300 R, Germany) equipped with a 785 nm laser for antimonene nanosheets and bulk Sb, and a Confocal Raman Microscope (Horiba LabRAM HR800) equipped with a 532 nm laser for bismuthene nanosheets and bulk Bi.

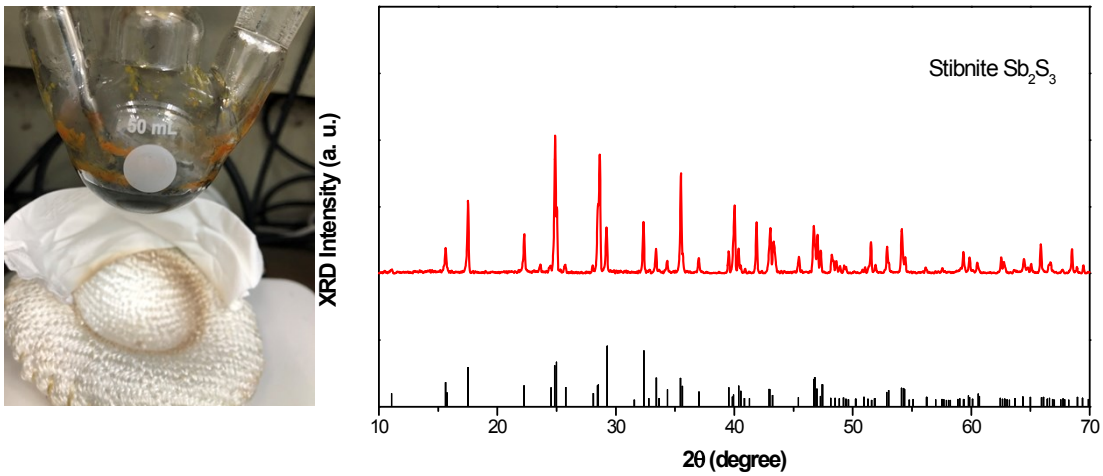

Figure S1. The photograph and XRD pattern of Sb_2S_3 synthesized by employing Sb-DDT as precursor at 300 °C.

The gray suspension formed accompany with orange precipitates appeared at the inner wall of the flask after Sb-DDT adding. XRD pattern of the obtained products suggests the formation of Sb_2S_3. The formation of Sb_2S_3 by-product is ascribed to the low thermal decomposition temperature of 1-DDT (~ 200 °C),[1,2] which caused sulfurization of the yielded monoelemental Sb.

(1) Y. Zhai, M. Shim, *Chem. Mater.* **2017**, *29*, 2390-2397;

(2) M. Kruszynska, H. Borchert, A. Bachmatiuk, M. H. Rümmeli, B. Büchner, J. Parisi, J. Kolny-Olesiak, *ACS Nano*, **2012**, *6*, 5889-5896.

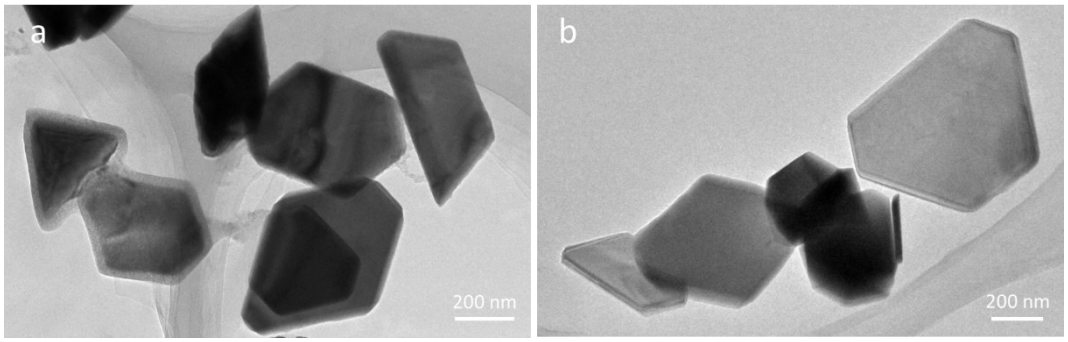

Figure S2-1. The TEM images of antimonene nanosheets synthesized at 250 °C for 1 min (a) and 230 °C for 20 min (b).

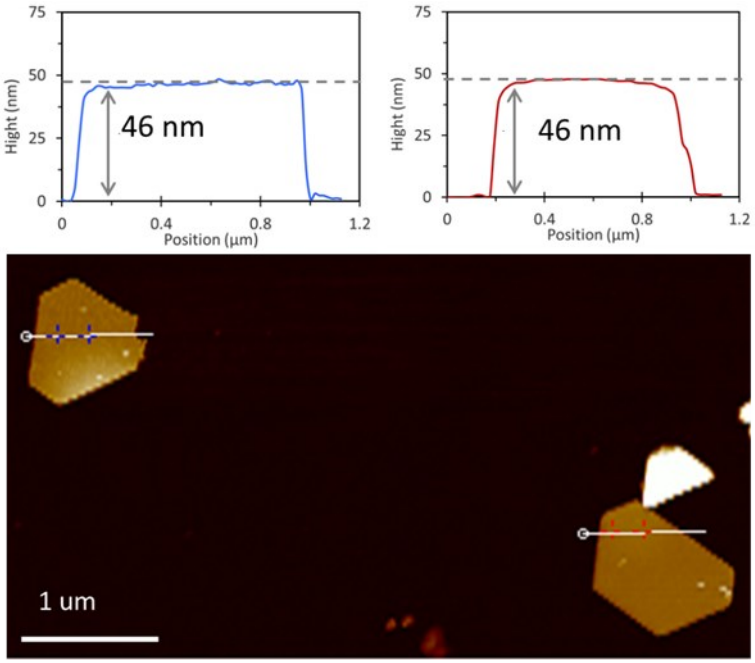

Figure S2-2. Typical AFM image and corresponding height profiles of synthesized antimonene nanosheet.

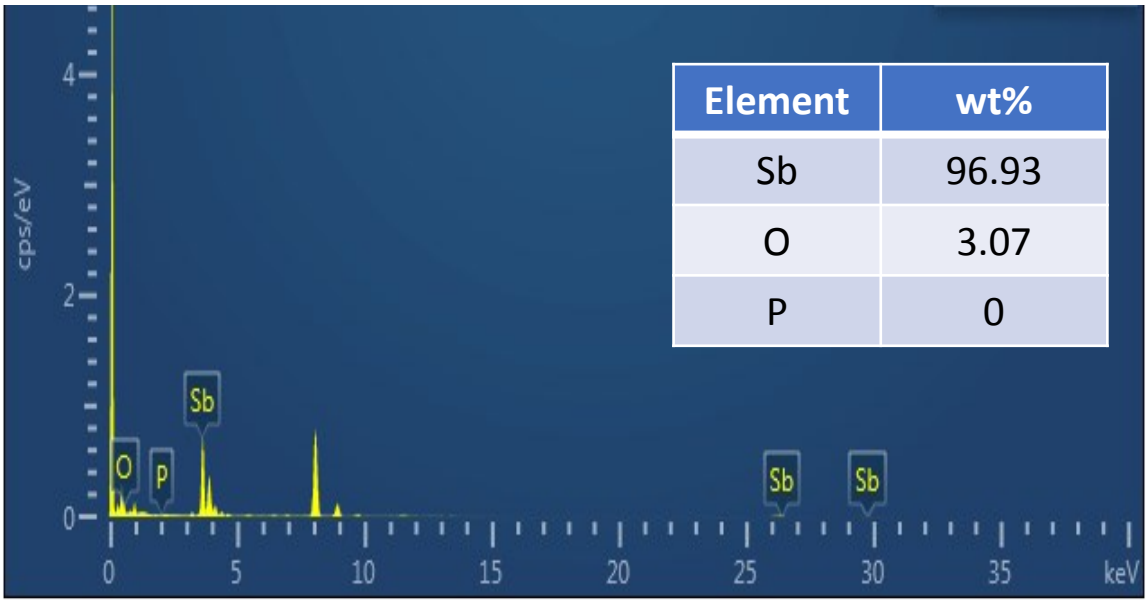

Element	wt%
Sb	96.93
O	3.07
P	0

Figure S2-3. EDS spectrum of the antimonene nanosheets. Here, the 0 wt% of P atom is attribute to the very trace amount of P atom which is below the detection limit of the machine.

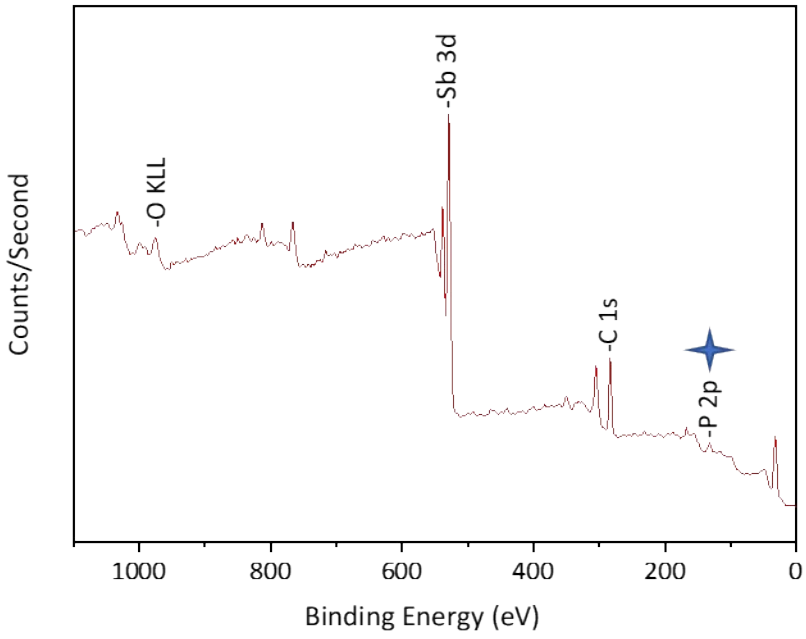

Figure S2-4. Wide-scan X-ray photoelectron spectra of the obtained antimonene nanosheets.

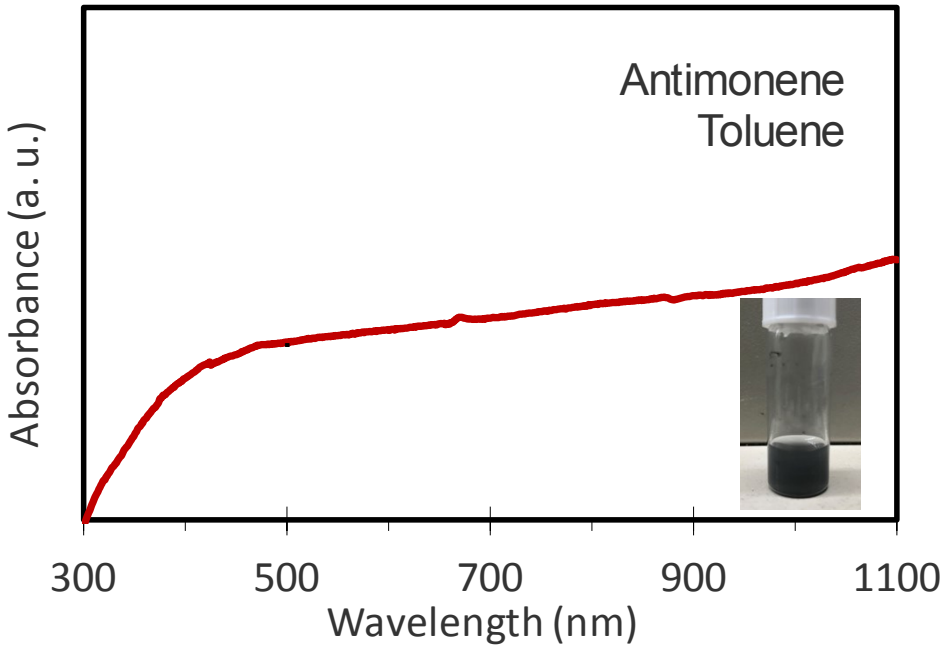

Figure S2-5. The absorption spectrum of the as-synthesized antimonene nanosheets, the photograph of antimonene solution dispersed in toluene is shown in the insert.

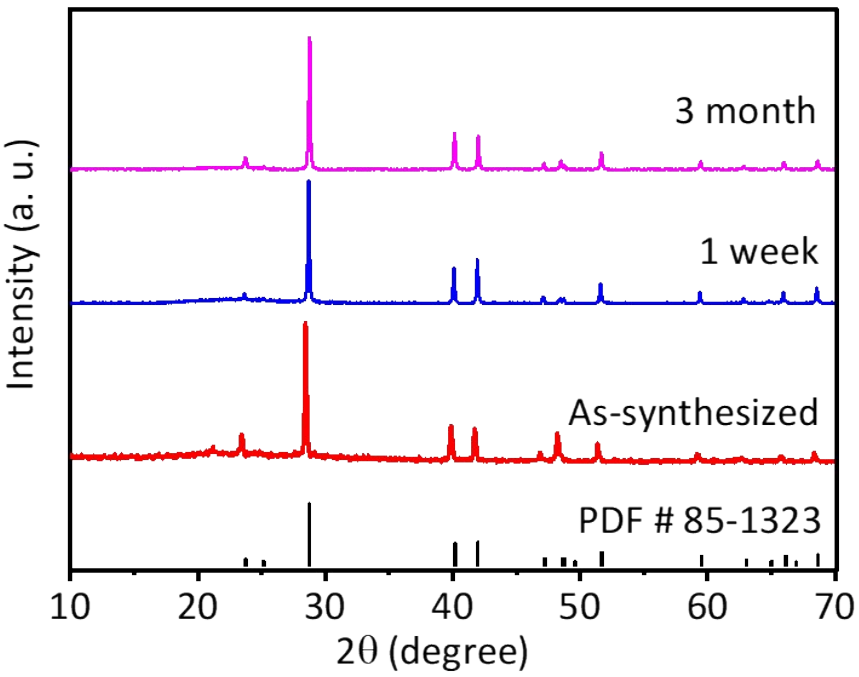

Figur

e S3-1. The XRD patterns of the as-synthesized antimonene nanosheets and after storage in the air.

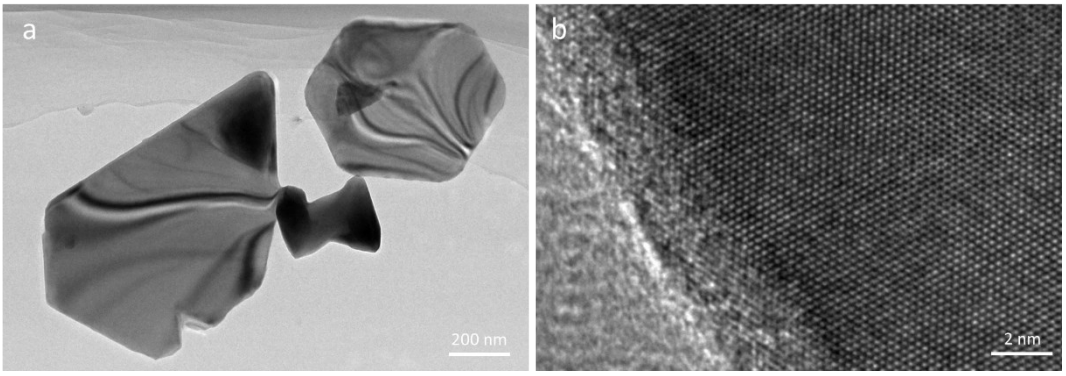

Figure S3-2. The TEM (a) and high-resolution TEM (b) images of antimonene nanosheets after storage for one week.

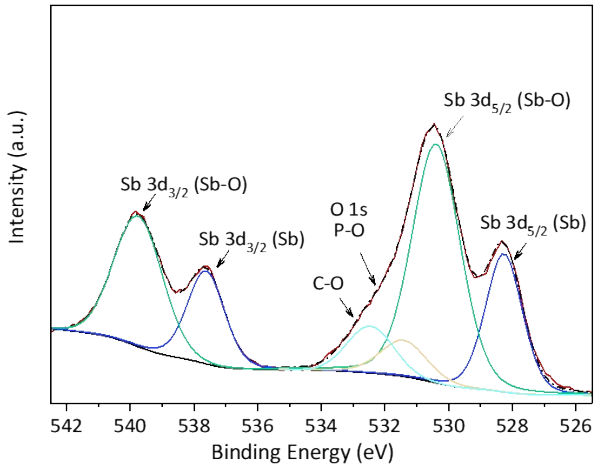

Figure S3-3. High-resolution XPS results and peak deconvolution of the as-synthesized antimonene nanosheets after storage for one week.

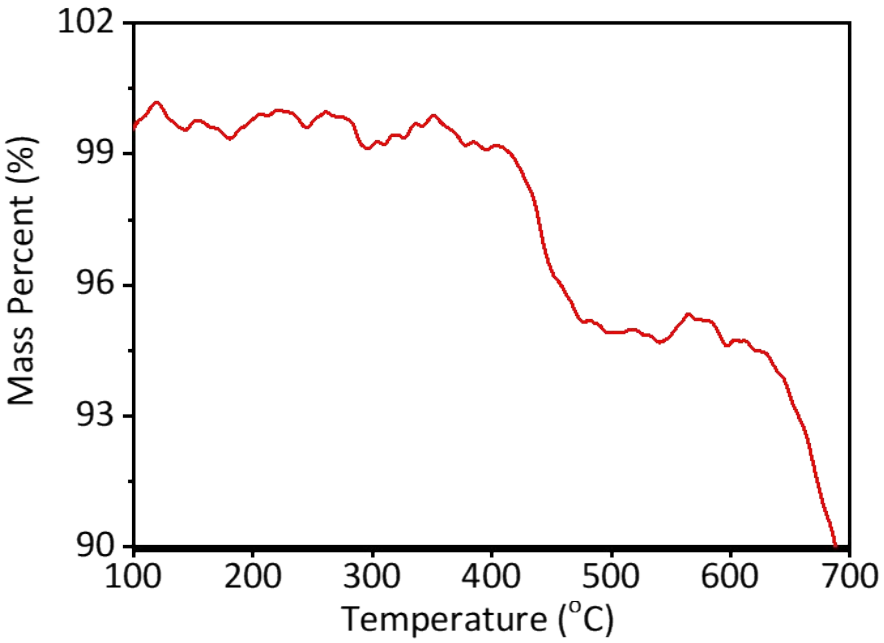

Figure S3-4. The TGA data of antimonene nanosheets.

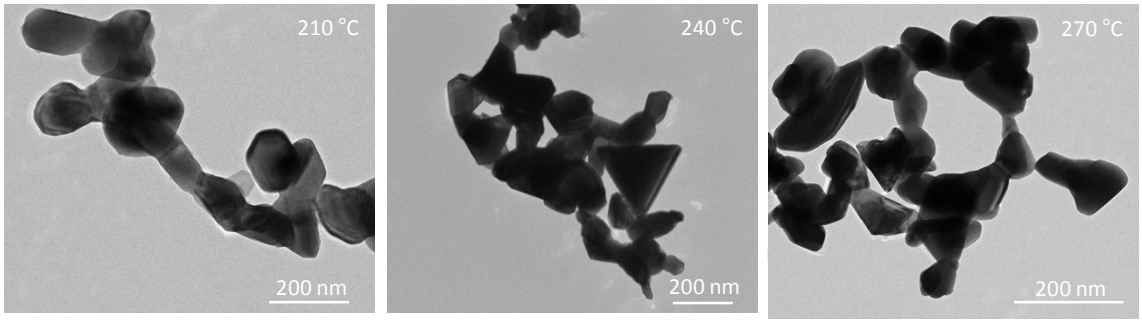

Figure S4-1. The TEM images of the sample extracted from the reaction of Sb-TOPO + OLA at 210 °C, 240 °C, and 270 °C. We consider that the precursor reactivity may change by using TOPO replaced of PA, thus the reaction was performed at a wide temperature range from 210 °C to 270 °C. Under all temperature conditions, irregular morphology was formed.

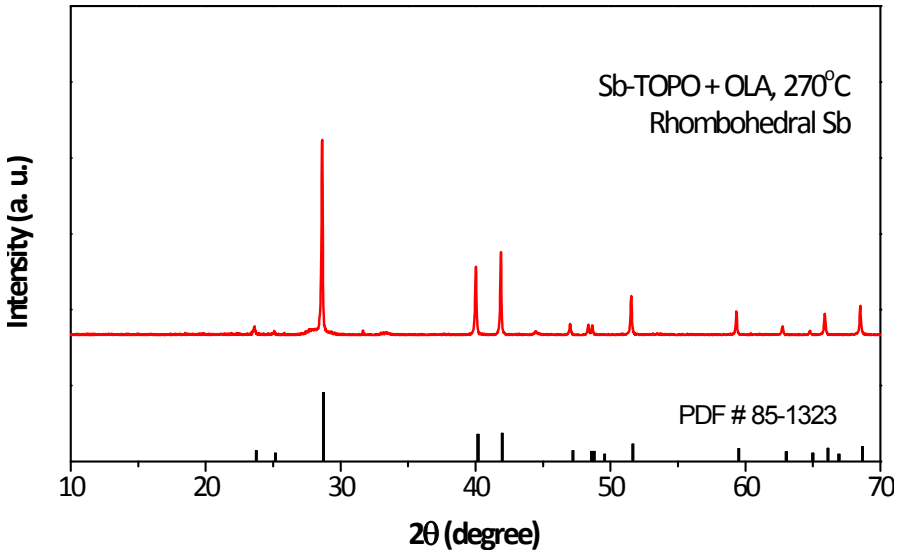

Figure S4-2. XRD pattern of the synthesized Sb nanocrystals from the reaction of Sb-TOPO + OLA at 270 °C. The obtained Sb nanocrystals shows a rhombohedral structure without the formation of Sb_2O_3.

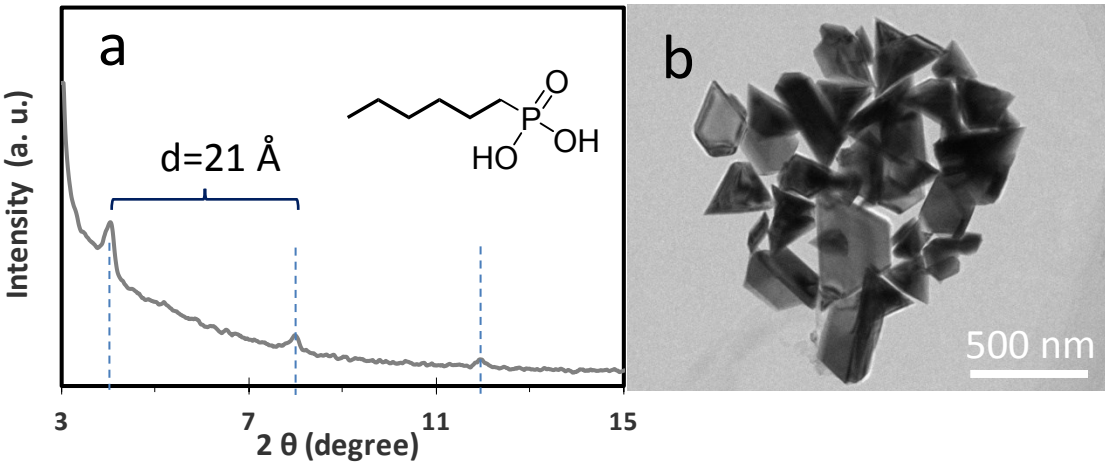

Figure S5-1. (a) The small angle XRD pattern of the Sb-HPA precursor and (b) the corresponding TEM image of antimonene nanosheets synthesized with Sb-HPA.

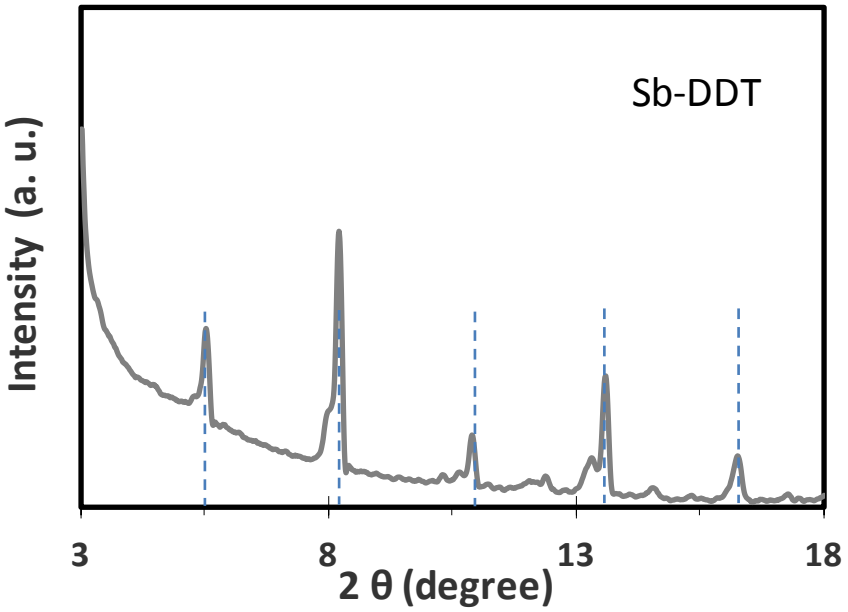

Figure S5-2. The small angle XRD pattern of the Sb-DDT precursor. The obviously uniformly-spaced diffraction peaks confirmed the formation of lamellar structure in Sb-DDT precursor. In order to get a solid powder for the XRD measurement, $Sb(OAc)_3$ was used instead of $SbCl_3$ for preparation of Sb-DDT precursor.

	Diffraction Peak (2Θ)	Average peak separation (2Θ)	Interlayer spacing (Å)	Ligand length (Å)
Sb-HPA	4.04/7.98/12.44	4.2	21.0	10.1
Sb-HDPA	4.2/6.34/8.48/10.6	2.13	41.4	21.8
Sb-TOPO	\	\	\	\
Sb-DDT	5.54/8.22/10.3/13.6/16.26	2.68	33.1	16.7

Table S1. Calculation of the interlayer spacing in the lamellar structure and the length of surface ligand molecule chains.

The interlayer spacing was calculated by $d=\lambda/2\sin\Theta$, where $\lambda=1.54$ Å, Θ is diffraction angle. The surface ligand length was calculated by an empirical formula, $L\ (nm) = 0.15 + 0.127n$, where n is the number of carbon atoms in the alkyl chain.[3]

(3) Evans, D. F.; Wennerström, H. The Colloidal Domain: Where Physics, Chemistry and Biology Meet; Wiley-VCH: Weinheim, 1999.

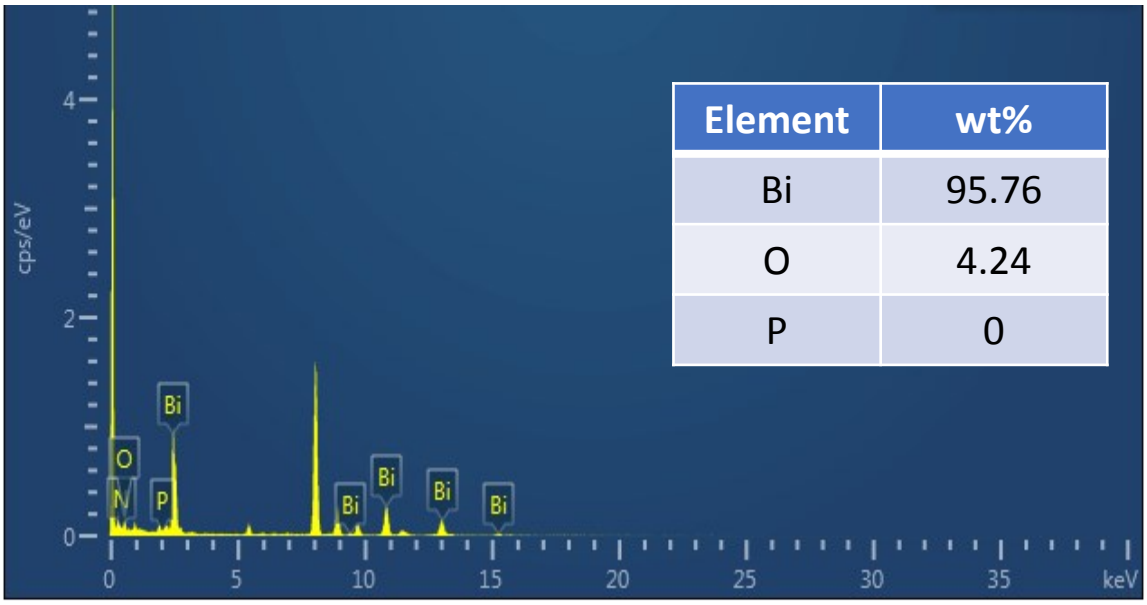

Element	wt%
Bi	95.76
O	4.24
P	0

Figure S6-1. EDS spectrum of the bismuthene nanosheets. Here, the 0 wt% of P atom is thanks to the very trace amount of P atom which is below the detection limit of the machine.

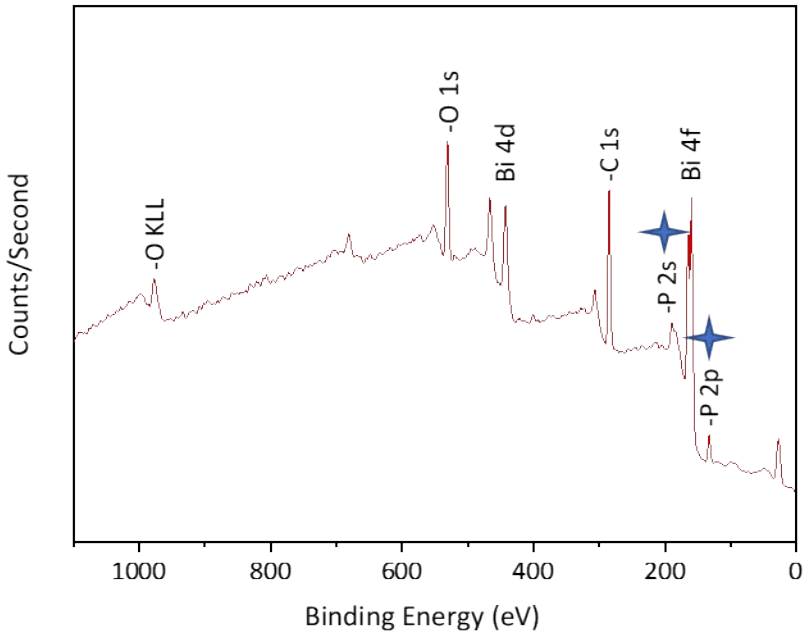

Figure S6-2. Wide-scan X-ray photoelectron spectra of the obtained bismuthene nanosheets.

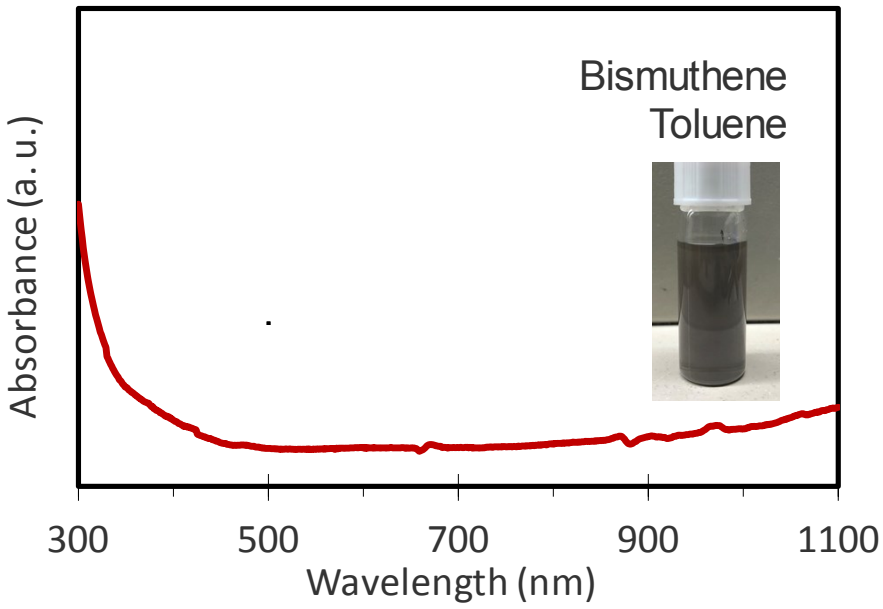

Figure S6-3. The absorption spectrum of the as-synthesized bismuthene nanosheets, the photograph of bismuthene solution dispersed in toluene is shown in the insert.

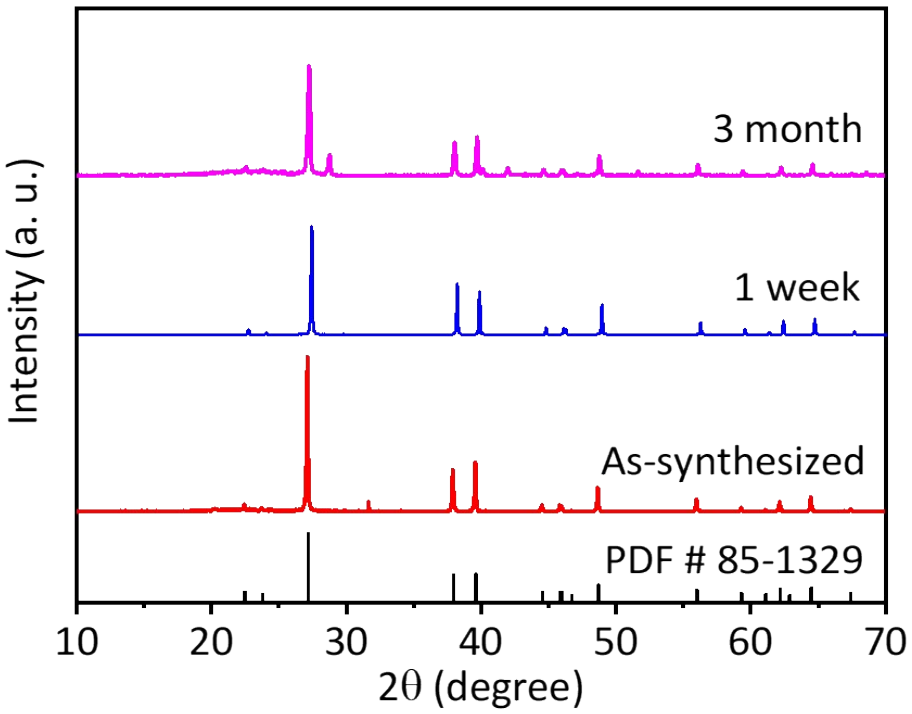

Figure S6-4. The XRD patterns of the as-synthesized bismuthene nanosheets and after storage in the air.